Multiphoton Rabi oscillations of a ringlike three-level system

Yong Lin He* and Jiu Ning Han

Department of Physics and Mechanical and Electrical Engineering, Hexi University, Zhangye Gansu 734000, People's Republic of China

(Received 15 February 2012; revised manuscript received 20 March 2012; published 17 April 2012)

We propose a ringlike three-level model and show that it can be realized using Stark states of highly excited potassium interacting with two-mode microwave fields. We demonstrate this by using both analytical model and numerical simulations to study the problems of multiphoton Rabi oscillations. The results show that the Rabi oscillation patterns of the ringlike three-level system exhibit additional envelope and nodes compared to the oscillatory behavior of a three-level cascade system; in other words, there exist collapse and revival phenomena for Rabi oscillation patterns. The origin of the collapse and revival of the population oscillations is the multiphoton two-color resonances at frequency $\Omega = n\omega_1 + m\omega_2$. Our analytic results are in good agreement with numerical simulations. In addition, all the analytical solutions for the three basic configurations of the three-level system classified as the Λ, vee, and cascade systems can be deduced from our analytical solution for the ringlike three-level configuration by setting one of the three coupling strengths equal to 0.

DOI: 10.1103/PhysRevA.85.043415 PACS number(s): 33.40.+f, 32.60.+i, 32.80.Rm, 32.30.Bv

I. INTRODUCTION

The three-level model is associated with a variety of physical processes, including electromagnetically induced transparency [1,2], stimulated Raman adiabatic passage [3,4], lasers without inversion [5,6], and laser cooling of atoms [7]. There has been increased interest in the study of three-level quantum systems, such as quantum computation [8] and quantum control [9,10]. Recently, it was found that photon blockade can be circumvented completely by using a three-level atom coupled to a single-sided cavity, enabling an ideal and robust photon routing mechanism [11].

Because of its basic importance, the exact solution of the three-level model to find the probability amplitudes of all three levels is required. There are three basic configurations of the three-level system, classified as the Λ, vee, and cascade systems. For the corresponding semiclassical models [12–14] and their fully quantized versions [15–17], the time dependence of the population can be described by explicit analytical expressions in the weak-coupling regime where the coupling strength between the atom and the fields is several orders of magnitude smaller than the frequencies of the fields. The collapses and revivals of the system populations due to the effect of field quantization are similar to the two level Jaynes-Cummings model [18–20]. It is worth pointing out that, despite its old age and central importance, the quantum Rabi model for a two-level system had never been solved exactly until it was declared solved for arbitrary coupling strength very recently [21].

For three-level systems, labeled $|1\rangle$, $|2\rangle$, and $|3\rangle$, of respective energies E_1, E_2, and E_3, driven by two resonant fields, under the rotating-wave and electric-dipole approximations and at zero detuning, the interaction Hamiltonian can be written as the Hermitian matrix

$$H = \begin{pmatrix} 0 & \Omega_{12} & \Omega_{13} \\ \Omega_{12} & 0 & \Omega_{23} \\ \Omega_{13} & \Omega_{23} & 0 \end{pmatrix}, \qquad (1)$$

where Ω_{ij} $(i,j = 1,2,3)$ represents the coupling strength between state $|i\rangle$ and state $|j\rangle$. Here we assume that the fields with real coupling strengths couple the atomic transitions. All the Hamiltonians for three basic configurations can be read off from Eq. (1) by setting one of the three coupling strengths equals 0. It is surprising that the general Hamiltonian of a three-level configuration with all the coupling strengths nonzero values has never been solved exactly. This situation has induced a closed, ringlike three-level configuration. To the best of our knowledge, no work has clearly concentrated on this ringlike three-level configuration.

Atoms in highly excited Rydberg states have very large electric dipole matrix elements for transitions to neighboring levels which scale as $d \sim qa_0n^2$, where q is the electron charge and a_0 the Bohr radius. For principal quantum number $n = 30$, the corresponding electric dipole matrix elements are about 3 orders of magnitude larger than those for low quantum numbers [22]. Study of atoms in highly excited Rydberg states interacting with external fields allows us to test fundamental theories on light-matter interaction. For example, an experiment on microwave multiphoton transitions between Stark states of highly excited potassium was done about 25 years ago [23]. A Stark state of highly excited potassium is labeled by its parabolic quantum number (n,n_1) [23]. It is not a state of definite parity because the wave function of the (n,n_1) state is the superposition of the wave functions of all zero-field states with the same n and $l \geqslant n_1$ due to the external static electric field. Single- or multiphoton resonances between Stark states of Rydberg potassium atoms occur when the separation between levels is equal to the integer times of the microwave frequency. Thus, the Stark states of highly excited potassium may serve as a good candidate for the considered ringlike three-level model.

In this paper, we report on the theoretical realization of the ringlike three-level configuration by investigating its multiphoton Rabi oscillation behavior. We derive the analytical solution for the ringlike three-level system using a nonperturbative resonant theory and the Laplace transform method. We also perform numerical simulations by solving the time-dependent Schrödinger equation. For numerical simulations, our ringlike three-level system consists of the (21,0), (19,3),

*hyl@hxu.edu.cn

and (19,4) Stark states of highly excited potassium. Our analytic results agree, qualitatively at least, with those of numerical simulations. It is found that the Rabi oscillation patterns of the ringlike three-level system are completely different from those of the Λ, vee, and cascade system; they exhibit additional envelope and nodes or collapse and revival phenomena due to the existence of the multiphoton two-color resonances at frequency $\Omega = n\omega_1 + m\omega_2$.

Our paper is organized as follows. In Sec. II we introduce the ringlike three-level model and derive its analytical solution. In Sec. III we perform numerical simulations by solving the time-dependent Schrödinger equation for highly excited potassium. We also show the comparison between the analytical solution and numerical simulations. Finally, conclusions are given in Sec. IV.

II. THEORETICAL MODEL AND ANALYTICAL SOLUTION

We consider a general model of two-mode microwave fields interacting with a three-level system as shown in Fig. 1. We assume that $|1\rangle \longleftrightarrow |2\rangle$, $|2\rangle \longleftrightarrow |3\rangle$, and $|1\rangle \longleftrightarrow |3\rangle$ transitions are all dipole allowed. We name this system the ringlike three-level system. For our ringlike three-level system, we assume that all three states are affected by the microwave fields. Then the interaction Hamiltonian for this system is presented in the form

$$\begin{aligned}\widehat{H} = {} & (\varepsilon_1 + V_{11})\,|1\rangle\langle 1| + (\varepsilon_2 + V_{22})\,|2\rangle\langle 2| \\ & + (\varepsilon_3 + V_{33})\,|3\rangle\langle 3| + (V_{12}\,|1\rangle\langle 2| \\ & + V_{23}\,|2\rangle\langle 3| + V_{13}\,|1\rangle\langle 3| + \text{H.c.}),\end{aligned} \tag{2}$$

where

$$V_{\text{ij}} = -d_{\text{ij}}(F_1\cos\omega_1 t + F_2\cos\omega_2 t) \tag{3}$$

and d_{ij} is the matrix element of the electric dipole moment. F_1 and F_2 are the amplitudes of the two microwave fields and ω_1 and ω_2 are the corresponding angular frequencies. V_{11}, V_{22}, and V_{33} account for interaction due to the mean dipole moments and these terms are important for the multiphoton resonance. The wave function of the system can be written in the form

$$\begin{aligned}|\psi(t)\rangle = {} & a_1(t)e^{-i(\varepsilon_1 t + \int_0^t V_{11}dt)}\,|1\rangle \\ & + a_2(t)e^{-i(\varepsilon_2 t + \int_0^t V_{22}dt)}\,|2\rangle \\ & + a_3(t)e^{-i(\varepsilon_3 t + \int_0^t V_{33}dt)}\,|3\rangle\,.\end{aligned} \tag{4}$$

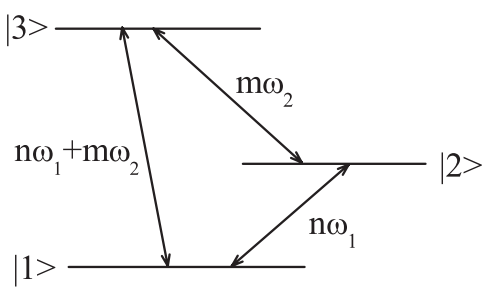

FIG. 1. Schematic for the ringlike three-level system. n and m are the numbers of photons.

From the time-dependent Schrödinger equation,

$$i\frac{\partial\,|\psi(t)\rangle}{\partial t} = \widehat{H}\,|\psi(t)\rangle\,, \tag{5}$$

and following the nonperturbative resonant approach introduced by Avetissian *et al.* [24,25], using the generalized rotating wave-approximation, and separating slow and rapid oscillations, we obtain the matrix equation for the time-average amplitudes with the assumption that fields with real coupling strengths couple atomic transitions,

$$i\frac{dX}{dt} = AX, \tag{6}$$

where

$$X = (\overline{a_1(t)},\overline{a_2(t)},\overline{a_3(t)})^T \tag{7}$$

is a column matrix,

$$A = \begin{pmatrix} -(\Delta_{12}+\Delta_{13}) & \Omega_{12}-\Lambda_{13,23} & \Omega_{13}+\Lambda_{12,23} \\ \Omega_{12}-\Lambda_{23,13} & \Delta_{12}-\Delta_{23} & \Omega_{23}+\Lambda_{23,12} \\ \Omega_{13}-\Lambda_{23,12} & \Omega_{23}+\Lambda_{13,12} & \Delta_{13}+\Delta_{23} \end{pmatrix}. \tag{8}$$

The coupling strengths are given by

$$\begin{aligned}\eta_{ij} = {} & -\frac{d_{ij}}{d_{jj}-d_{ii}}(s_1\omega_1 + s_2\omega_2)J_{s_1}\left[(d_{jj}-d_{ii})\frac{F_1}{\omega_1}\right] \\ & \times J_{s_2}\left[(d_{jj}-d_{ii})\frac{F_2}{\omega_2}\right], \quad i,j = 1,2,3,\end{aligned} \tag{9}$$

where J_{s_1} and J_{s_2} are the Bessel functions of the first kind with orders s_1 and s_2, respectively. For simplicity, we only consider the case where the resonant condition holds for any pair of photon numbers $\{s_1 = n, s_2 = m\}$, single-channel resonance; then the terms $\Omega_{ij} = \eta_{ij}(n,m)$ $(i,j = 1,2,3)$ represent the coupling strengths or the generalized Rabi frequencies related to n and m photons. The terms Δ_{ij} and $\Lambda_{ij.kl}$ $(i,j,k,l = 1,2,3)$ describe dynamic Stark shifts, which can be written as follows:

$$\Delta_{ij} = \sum_{s_1\neq n}\sum_{s_2\neq m}\frac{\eta_{ij}(n,m)\eta_{ij}(s_1,s_2)}{(s_1-n)\omega_1 + (s_2-m)\omega_2}, \tag{10}$$

$$\Lambda_{ij,kl} = \sum_{s_1\neq n}\sum_{s_2\neq m}\frac{\eta_{ij}(n,m)\eta_{kl}(s_1,s_2)}{(s_1-n)\omega_1 + (s_2-m)\omega_2}. \tag{11}$$

At the exact resonance, while all the dynamic Stark shifts become 0, matrix A is reduced to the real symmetric matrix H given by Eq. (1); then the analytical solution to Eq. (6) is found by applying the approach of Laplace transform when the generalized Rabi frequency is much less than the electromagnetic waves periods. The analytical solution for the system situated initially in state $|1\rangle$ is

$$\begin{aligned}\overline{a_j(t)} = {} & \rho_{j1}\exp\left[\frac{\left(2^{\frac{1}{3}}\alpha^{\frac{2}{3}} - 6\gamma\right)t}{3\times 2^{\frac{2}{3}}\alpha^{\frac{1}{3}}}\right] \\ & + \rho_{j2}\exp\left\{\frac{\left[-2^{\frac{1}{3}}\alpha^{\frac{2}{3}} + 6\gamma - \sqrt{3}\left(-6\Omega_{12}^2 + 2^{\frac{1}{3}}\alpha^{\frac{2}{3}} + 6\gamma\right)i\right]t}{6\times 2^{\frac{2}{3}}\alpha^{\frac{1}{3}}}\right\}\left[\cos\left(\frac{\sqrt{3}\Omega_{12}^2 t}{2^{\frac{2}{3}}\alpha^{\frac{1}{3}}}\right) - i\sin\left(\frac{\sqrt{3}\Omega_{12}^2 t}{2^{\frac{2}{3}}\alpha^{\frac{1}{3}}}\right)\right] \\ & - \rho_{j3}\exp\left\{\frac{[(-1)^{\frac{2}{3}}2^{\frac{1}{3}}\alpha^{\frac{2}{3}} + 3\gamma + 3\sqrt{3}(-\Omega_{12}^2 + \gamma)i]t}{3\times 2^{\frac{2}{3}}\alpha^{\frac{1}{3}}}\right\}\left[\cos\left(\frac{\sqrt{3}\Omega_{12}^2 t}{2^{\frac{2}{3}}\alpha^{\frac{1}{3}}}\right) + i\sin\left(\frac{\sqrt{3}\Omega_{12}^2 t}{2^{\frac{2}{3}}\alpha^{\frac{1}{3}}}\right)\right], \\ & j = 1,2,3,\end{aligned} \tag{12}$$

where we have introduced the following parameters:

$$\delta = \Omega_{12}\Omega_{13}\Omega_{23}, \tag{13}$$

$$\gamma = \Omega_{12}^2 + \Omega_{13}^2 + \Omega_{23}^2, \tag{14}$$

$$\beta = \sqrt{-27\delta^2 + \gamma^3}, \tag{15}$$

$$\alpha = 54\delta i + \sqrt{-2196\delta^2 + 108\gamma^3} \tag{16}$$

and

$$\rho_{11} = \frac{2^{\frac{4}{3}}\left[(-2\gamma + 3\Omega_{23})\alpha^{\frac{2}{3}} + 3\times 2^{\frac{2}{3}}\gamma^2 + 2^{\frac{1}{3}}\sqrt{3}\beta\alpha^{\frac{1}{3}} + 9\times 2^{\frac{1}{3}}\delta\alpha^{\frac{1}{3}}i\right]}{2^{\frac{2}{3}}\alpha^{\frac{4}{3}} - 6\times 2^{\frac{1}{3}}\alpha^{\frac{2}{3}}\gamma + 36\gamma^2}, \tag{17}$$

$$\rho_{12} = \frac{2^{\frac{4}{3}}\sqrt{3}\left\{2\alpha^{\frac{2}{3}}\left(2\gamma - 3\Omega_{23}^2\right) + (-1)^{\frac{1}{3}}6\times 2^{\frac{2}{3}}\gamma^2 + 2^{\frac{1}{3}}\alpha^{\frac{1}{3}}[\sqrt{3}(\beta + 9\delta) - 3(\beta - 3\delta)i]\right\}}{(2^{\frac{1}{3}}\alpha^{\frac{2}{3}} + 6\gamma)[2^{\frac{1}{3}}\alpha^{\frac{2}{3}}(\sqrt{3} - 3i) - 6\gamma(\sqrt{3} + 3i)]}, \tag{18}$$

$$\rho_{13} = \frac{2^{\frac{4}{3}}\sqrt{3}\left\{-2\alpha^{\frac{2}{3}}\left(2\gamma - 3\Omega_{23}^2\right) + 6\times(-2)^{\frac{2}{3}}\gamma^2 - 2^{\frac{1}{3}}\alpha^{\frac{1}{3}}[\sqrt{3}(\beta - 9\delta) + 3(\beta + 3\delta)i]\right\}}{\sqrt{3}(2^{\frac{1}{3}}\alpha^{\frac{2}{3}} + 6\gamma)^2 + 3(2^{\frac{2}{3}}\alpha^{\frac{4}{3}} - 36\gamma^2)i}, \tag{19}$$

$$\rho_{21} = \frac{-6\times 2^{\frac{1}{3}}\Omega_{13}\Omega_{23}\alpha^{\frac{2}{3}} + 108\Omega_{12}\delta - 6\Omega_{12}\left(2\sqrt{3}\beta - 2^{\frac{2}{3}}\alpha^{\frac{1}{3}}\gamma\right)i}{2^{\frac{2}{3}}\alpha^{\frac{4}{3}} - 6\times 2^{\frac{1}{3}}\alpha^{\frac{2}{3}}\gamma + 36\gamma^2}, \tag{20}$$

$$\rho_{22} = \frac{12\sqrt{3}\left(2^{\frac{1}{3}}\Omega_{13}\Omega_{23}\alpha^{\frac{2}{3}} + 9\Omega_{12}\delta + 3\Omega_{12}\beta\right) - 12\Omega_{12}\left[3\beta + (-2)^{\frac{2}{3}}\sqrt{3}\alpha^{\frac{1}{3}}\gamma - 27\delta\right]i}{\sqrt{3}(2^{\frac{1}{3}}\alpha^{\frac{2}{3}} + 6\gamma)^2 - 3(2^{\frac{2}{3}}\alpha^{\frac{4}{3}} - 36\gamma^2)i}, \tag{21}$$

$$\rho_{23} = \frac{12\sqrt{3}\left[3\Omega_{12}\beta - 2^{\frac{1}{3}}\Omega_{13}\Omega_{23}\alpha^{\frac{2}{3}} - (-1)^{\frac{5}{6}}2^{\frac{2}{3}}\Omega_{12}\alpha^{\frac{1}{3}}\gamma\right] + 36\Omega_{12}(9\delta + \beta)i}{\sqrt{3}(2^{\frac{1}{3}}\alpha^{\frac{2}{3}} + 6\gamma)^2 + 3(2^{\frac{2}{3}}\alpha^{\frac{4}{3}} - 36\gamma^2)i}, \tag{22}$$

$$\rho_{31} = \frac{-2^{\frac{1}{3}}\Omega_{12}\Omega_{23}\alpha^{\frac{2}{3}} + 18\Omega_{13}\delta - \Omega_{13}\left(2\sqrt{3}\beta - 2^{\frac{2}{3}}\alpha^{\frac{1}{3}}\gamma\right)i}{\frac{1}{6}\times 2^{\frac{2}{3}}\alpha^{\frac{4}{3}} - 2^{\frac{1}{3}}\alpha^{\frac{2}{3}}\gamma + 6\gamma^2}, \tag{23}$$

$$\rho_{32} = \frac{6\times(-2)^{\frac{2}{3}}\sqrt{3}\Omega_{13}\alpha^{\frac{1}{3}}\gamma - 162\Omega_{13}\delta + 18\Omega_{13}\beta + 6\sqrt{3}\left(3\Omega_{13}\beta + 2^{\frac{1}{3}}\Omega_{12}\Omega_{23}\alpha^{\frac{2}{3}} + 9\Omega_{13}\delta\right)i}{\{\sqrt{3}[(-1)^{\frac{1}{6}}2^{\frac{1}{3}}\alpha^{\frac{2}{3}} + 3\gamma i] - 9\gamma\}(2^{\frac{1}{3}}\alpha^{\frac{2}{3}} + 6\gamma)}, \tag{24}$$

$$\rho_{33} = \frac{12\sqrt{3}\left\{2^{\frac{1}{3}}\Omega_{12}\Omega_{23}\alpha^{\frac{2}{3}} + \Omega_{13}\left[-3\beta + (-1)^{\frac{5}{6}}2^{\frac{2}{3}}\alpha^{\frac{1}{3}}\gamma + 9\delta\right]\right\} + 108\sqrt{3}\Omega_{13}\delta - 36\Omega_{13}(9\delta + \beta)i}{\sqrt{3}(2^{\frac{1}{3}}\alpha^{\frac{2}{3}} + 6\gamma)^2 + 3\left(2^{\frac{2}{3}}\alpha^{\frac{4}{3}} - 36\gamma^2\right)i}. \tag{25}$$

The analytical solution, Eq. (12) describes oscillations of the probability amplitudes for the ringlike three-level system analogously to ordinary Rabi oscillations.

III. NUMERICAL RESULTS AND DISCUSSION

In this section, we show that the ringlike three-level configuration can be realized using Stark states of highly excited potassium interacting with two-mode microwave fields. To do this, it is essential to examine the reliability of the predictions obtained from our ringlike three-level model. We test the model by numerical experiment. Therefore, we focus on the study of the transient dynamics of the ringlike three-level configuration. Calculations of the population of the three states using both the analytical solution, Eq. (12) and numerical simulations are performed. As an example, we take the three Stark states of highly excited potassium: $|1\rangle = (21,0)$, $|2\rangle = (19,3)$, and $|3\rangle = (19,4)$. The Stark electric dipole moments are the bridge leading to quantitative comparison between analytical results and corresponding numerical results. In numerical simulation, we employ the time-dependent close-coupling (TDCC) method to solve the time-dependent Schrödinger equation. The details of the TDCC method used in the simulations are given in Refs. [26–31]. For the numerical simulations reported here, we use both the three-state approximation (TSA) of TDCC and the multistate description (MSD) of TDCC. In TSA, only the three essential states, (21,0), (19,3) and (19,4), are included. The results of the MSD are the calculated Rabi frequencies of the multiphoton resonances from the (21,0) to the (19,2 $\sim$ 18) Stark states; the grand total of 18 states that straddles the (21,0), (19,3), and (19,4) states is included in the calculation. The MSD is considered to rely more on the real behavior of the potassium atom. The analytical simulations are performed under our excitation conditions for the corresponding numerical simulations; the Stark electric dipole moments used to calculate the coupling strength are determined by the Stark state wave functions $\psi_k^{(s)}$. Within the electric dipole approximation, the Stark electric dipole moment d_{ij} may be written in the following form [30,31]:

$$d_{\rm ij} = \langle \psi_i^{(s)} | P^{(1)} | \psi_j^{(s)} \rangle = \langle \psi_i^{(s)} | {\rm rC}_0^{(1)} | \psi_j^{(s)} \rangle \qquad (26)$$

The Stark states wave functions are obtained by the diagonalizing the Stark Hamiltonian with the B-spline basis [30,31]. In Table I, we list the values of Stark electric dipole moments for the (21,0), (19,3), and (19,4) Stark states of highly excited potassium with a static electric amplitude equal to 286.32 V/cm.

Figure 2 shows the temporal evolution of the three states' populations at $\omega_1/2\pi = 9.0$ GHz, $F_1 = 10$ V/cm and $\omega_2/2\pi = 26.16$ GHz, $F_2 = 10$ V/cm, with a static-field amplitude equal to 286.32 V/cm. Both the results of the MSD and the results of the analytical solution, Eq. (12) are displayed. In Fig. 2(c), the results of the TSA are also displayed. In the analytical simulations, the generalized Rabi frequencies are decided by Eq. (9) and the dynamic Stark shifts are calculated by Eqs. (10) and (11). All related values are listed in Table II. As show, the dynamic Stark shifts are much less than the generalized Rabi frequencies. In order to check whether the dynamic Stark shifts can be safely neglected, we solve Eq. (6) numerically with the dynamic Stark shifts included by using the Runge-Kutta algorithm; comparison with the results of the analytical solution, Eq. (12) show that dynamic Stark shifts can be safely neglected. One can note that the Rabi

TABLE I. Calculated Stark electric dipole moments $|d_{ij}|$, in atomic units.

	$i = 1$	$i = 2$	$i = 3$
$j = 1$	44.564	8.604	3.026
$j = 2$	8.604	467.607	12.158
$j = 3$	3.026	12.158	399.948

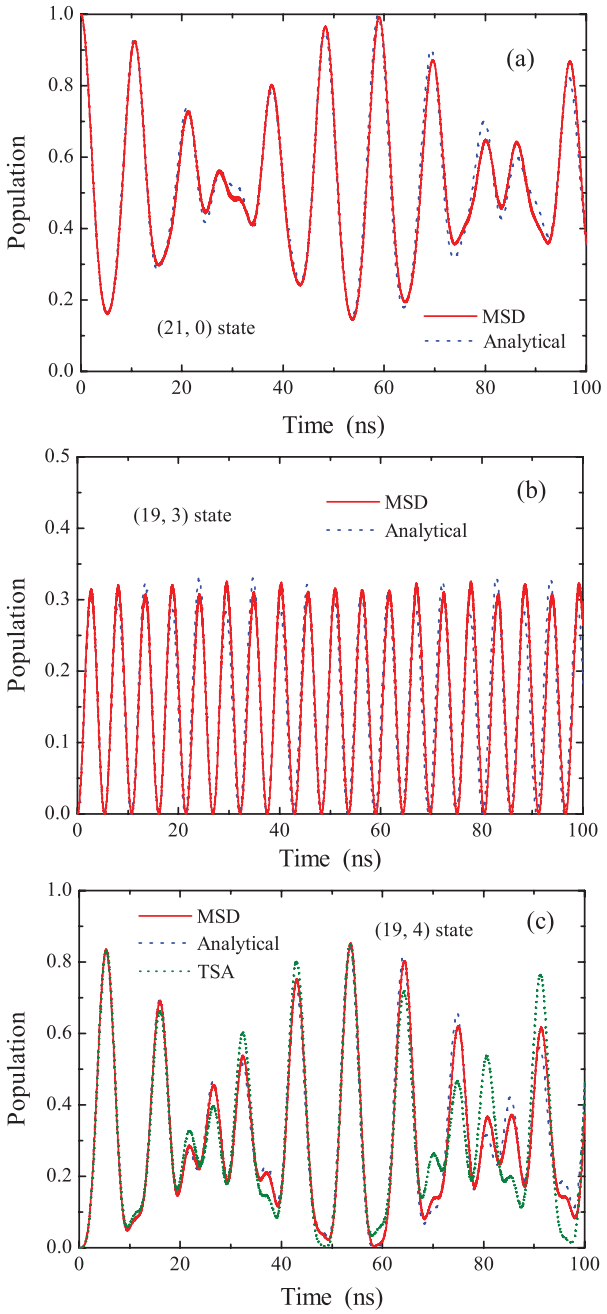

FIG. 2. (Color online) Comparison of the populations of (a) (21,0), (b) (19,3), and (c) (19,4) states between the numerical solution of the time-dependent Schrödinger equation using the MSD of TDCC [solid (red) line], the TSA [dotted (green) line], and the analytical solution [dashed (blue) line] at $\omega_1/2\pi = 9.0$ GHz, $F_1 = 10$ V/cm, and $\omega_2/2\pi = 26.16$ GHz, $F_2 = 10$ V/cm, with a static field amplitude equal to 286.32 V/cm.

TABLE II. Calculated generalized Rabi frequencies and dynamic Stark shifts (in MHz) and amplitudes of microwave fields F_1 and F_2 (inV/cm).

	$(n,m) = (1,1)$ $F_1 = 10$ $F_2 = 10$	$(n,m) = (2,1)$ $F_1 = 15$ $F_2 = 6$
Ω_{12}	5.198×10^{1}	5.594×10^{1}
Ω_{13}	6.349×10^{0}	3.684×10^{0}
Ω_{23}	7.760×10^{1}	4.570×10^{1}
Δ_{12}	1.177×10^{-3}	-1.170×10^{-2}
Δ_{13}	5.245×10^{-3}	5.640×10^{-3}
Δ_{23}	5.418×10^{-1}	4.444×10^{-1}
$\Lambda_{13,23}$	4.433×10^{-2}	3.582×10^{-2}
$\Lambda_{12,23}$	3.629×10^{-1}	5.440×10^{-1}
$\Lambda_{23,13}$	6.410×10^{-2}	6.997×10^{-2}
$\Lambda_{12,13}$	4.294×10^{-2}	8.565×10^{-2}
$\Lambda_{23,12}$	1.757×10^{-3}	-9.565×10^{-3}
$\Lambda_{13,12}$	1.438×10^{-4}	-7.709×10^{-4}

oscillation behaviors predicted by our analytical solution agree quantitatively with those of the numerical results of the MSD. The dotted (green) curve in Fig. 2(c) shows the results of the TSA. The Rabi oscillation patterns are consistent qualitatively despite the apparent quantitative differences between the MSD and the TSA results. Usually, the MSD of TDCC is considered more accurate compared to the TSA of TDCC. Here, we show that the results of the TSA are also reliable. All the above results and analyses allow us to predict that two-photon two-color resonance at frequency $\Omega = n\omega_1 + m\omega_2$, with $n = 1$, $m = 1$, occurs between the (21,0) and the (19,4) Stark states of highly excited potassium.

Figure 3 displays the temporal evolution of the three states' populations at $\omega_1/2\pi = 4.5$ GHz, $F_1 = 15$ V/cm and $\omega_2/2\pi = 26.16$ GHz, $F_2 = 6$ V/cm, with a static electric field amplitude equal to 286.32 V/cm; the results of the analytical solution are also displayed. The generalized Rabi frequencies and dynamic Stark shifts are also listed in Table II. We see apparent quantitative differences, however, our analytic results agree, qualitatively at least, with the numerical results. In this situation, it allows us to predict that three-photon two-color resonance at frequency $\Omega = n\omega_1 + m\omega_2$, with $n = 2$, $m = 1$, occurs between the (21,0) and the (19,4) Stark states of highly excited potassium.

In Figs. 2 and 3, we find that the population oscillations exhibit an additional envelope and nodes compared to the oscillatory behavior of a three-level cascade system [20]. The oscillation patterns strongly resemble the collapse and revival effect known from quantum optics due to field quantization. The main difference between the ringlike three-level system and the cascade-type system is the existence of $|1\rangle \longleftrightarrow |3\rangle$ multiphoton two-color resonance. It is just the $|1\rangle \longleftrightarrow |3\rangle$ multiphoton two-color resonance that leads to the appearance of the additional envelope and nodes or the collapse and revival phenomena. Therefore, the nature of the collapse and revival phenomena is different from that of the Jaynes-Cummings model.

Figure 4 displays the dependence of the Rabi oscillations of three-photon two-color resonance for our ringlike

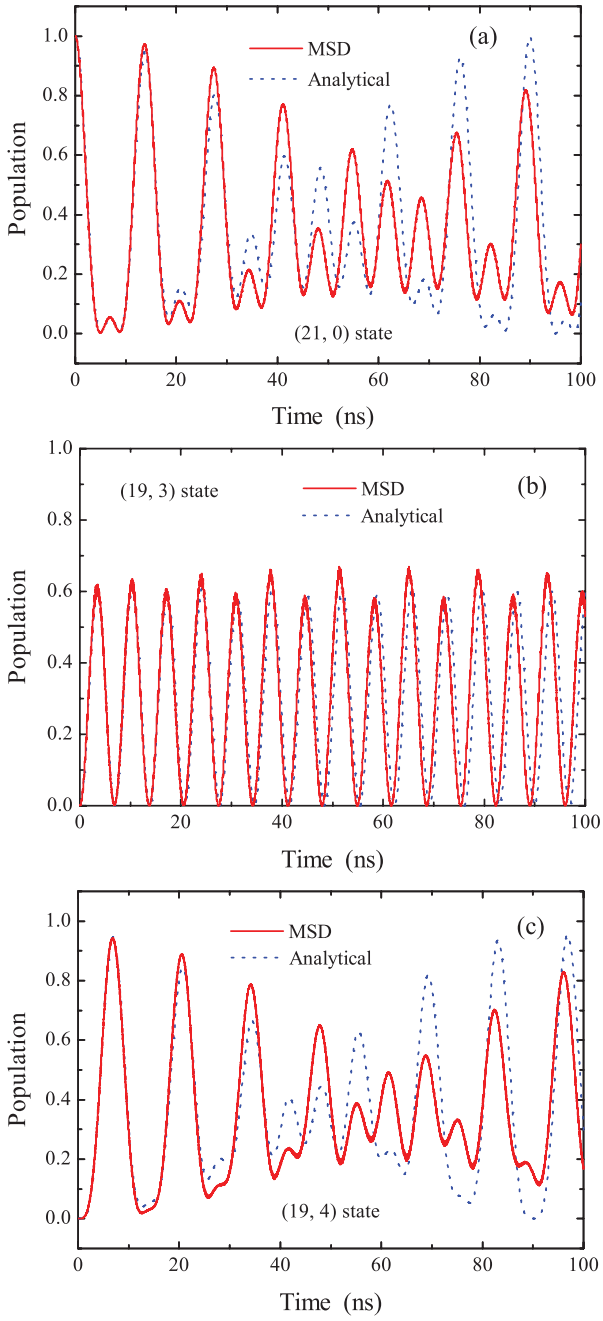

FIG. 3. (Color online) Comparison of the populations of (a) (21,0), (b) (19,3), and (c) (19,4) between the numerical solution of the time-dependent Schrödinger equation using the MSD of TDCC [solid (red) line] and the analytical solution [dashed (blue) line] at $\omega_1/2\pi = 4.5$ GHz, $F_1 = 15$ V/cm and $\omega_2/2\pi = 26.16$ GHz, $F_2 = 6$ V/cm, with a static field amplitude equal to 286.32 V/cm.

three-level system on the amplitudes of the microwave field. For these simulations, keeping $F_1 = 15$ V/cm fixed and setting $\omega_1/2\pi = 4.5$ GHz, and $\omega_2/2\pi = 26.16$ GHz, we obtain the Rabi oscillation behavior for various amplitudes of F_2. The oscillation behavior of the three levels is calculated using Eq. (6), while dynamic Stark shifts are neglected. The coupling strengths $\Omega_{ij} = \eta_{ij}(n,m)$ $(i,j = 1,2,3)$ are calculated using the Stark electric dipole moments listed in Table I. At the lower amplitudes of F_2, only resonance between the (21,0) and the

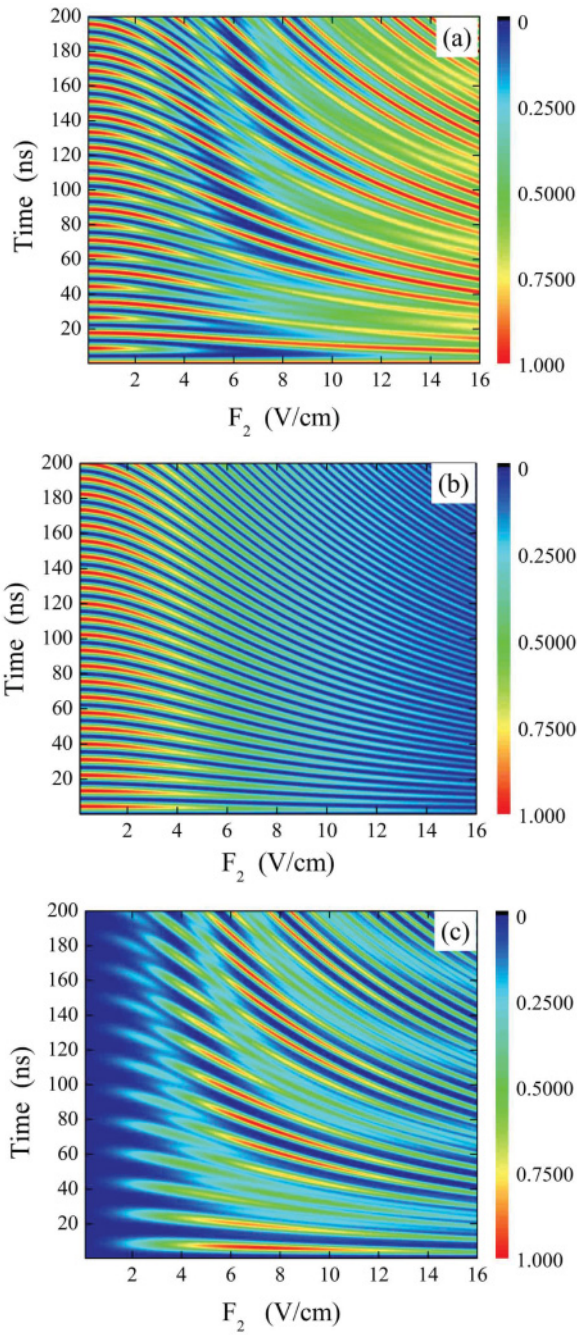

FIG. 4. (Color online) Contour plot of the population as a function of the amplitude of the driving microwave field F_2 and the tome. Parameters employed are $F_1 = 15$ V/cm, $\omega_1/2\pi = 4.5$ GHz, and $\omega_2/2\pi = 26.16$ GHz. (a) Oscillations for the (21,0) state, which is connected to the initial state; corresponding simulations for the (b) (19,3) and (c) (19,4) states.

(19,3) states occur, giving no resonant transition of (19,3) → (19,4) and (21,0) → (19,4). At higher amplitudes of F_2 (e.g., 4–12 V/cm), either (21,0) → (19,3) or (19,3) → (19,4) and (21,0) → (19,4) transitions occur. With an increase in the amplitudes of F_2, all the resonances finally disappear. The distinct feature is that there is a banded structure in Fig. 4 for the ringlike three-level system. The banded structure for (21,0) and (19,4) states reflects the the collapse and revival behavior. Thus the multiphoton two-color resonance between the (21,0) and the (19,4) states plays a critical role in determining the character of the banded structure. However, Figs. 2(b) and 3(b) show that there are almost no additional envelope and nodes or collapse and revival behavior for (19,3) state. Accordingly, there is no banded structure in Fig. 4(b) for the (19,3) state. Note that the corresponding results for two-photon two-color resonance are similar to those for three-photon two-color resonance. Therefore, the ringlike three-level configuration can be realized only for a narrow range of parameters.

Note that the resonance condition can also be satisfied by diverse pairs of photon numbers; if the microwave frequency is far less than the separation between the levels, then there are many channels of resonance transitions and one should take into account all possible transitions. In this case, it is difficult to show quantitative agreement between analytic results and numerical simulations. Thus, we restrict our simulations to the situation of single-channel resonance.

The ringlike three-level model exists and is valid because it has given results in accord with numerical simulations. The validity can be further checked in the following way. If the coupling strength Ω_{23} equals 0 in Eq. (12), then our analytical solution can be reduced to the analytical solution for the vee-configuration three-level system. This is also true for the Λ and cascade configurations when the coupling strength Ω_{12} or Ω_{13} equals 0 in Eq. (12).

IV. CONCLUSION

In this paper we have proposed a ringlike three-level model. We have studied the Rabi oscillations of multiphoton transitions in the ringlike three-level system interacting with two-mode microwave fields both numerically and analytically. The analytical solution for the description of the time-dependent atomic population of the three states for the ringlike three-level system is found by using the nonperturbative resonant approach and the method of Laplace transform. We make numerical simulations by directly solving the time-dependent Schrödinger equation, Eq. (5) using both the MSD of the TDCC method and the TSA of the TDCC method. In the numerical simulations, the ringlike three-level system consists of the (21,0), (19,3), and (19,4) Stark states of highly excited potassium. Our analytic results for two-photon two-color resonance agree quantitatively with those of numerical solutions of the time-dependent Schrödinger equation. For the case of three-photon two-color resonance, qualitative agreement is observed. The results show that the Rabi oscillation patterns of the ringlike three-level system are completely different from those of the Λ, vee, and cascade systems: they exhibit additional envelope and nodes compared to the oscillatory behavior of the three-level cascade system; in other words, collapse and revival phenomena exist. The $|1\rangle \longleftrightarrow |3\rangle$ multiphoton two-color resonance at frequency $\Omega = n\omega_1 + m\omega_2$ leads to the appearance of the collapse and revival phenomena. The contour plot of populations as a function of the amplitude of the driving microwave field F_2 and the time exhibits banded structures which reflect the collapse and revival phenomena of the system populations. Again, the origin of the banded structures is the multiphoton two-color resonance between the (21,0) and the (19,4) states.

Our results allows us to conclude that the ringlike three-level configuration can be realized using Stark states of highly excited potassium for a narrow range of parameters. The ringlike three-level configuration may be found and studied in other, more accessible systems. The validity of any model resides in its agreement with experiment. Equation (12) forms part of a new three-level configuration; we hope that our ringlike three-level model stimulates experiments.

ACKNOWLEDGMENTS

This work was supported by the Young Teachers Scientific Research Fund Project of He Xi University under Grant No. QN2011-14 and the Youth Science and Technology Research Projects Foundation of Gansu Province of China. Y.L.H. gratefully acknowledges the help from Professor Xiao-Xin Zhou and is grateful to Dr. Cheng Jin for help with numerical methods and useful discussions.

[1] D. J. Fulton, S. Shepherd, R. R. Moseley, B. D. Sinclair, and M. H. Dunn, Phys. Rev. A **52**, 2302 (1995).
[2] Y. Q. Li and M. Xiao, Phys. Rev. A **51**, R2703 (1995).
[3] K. Bergmann, H. Theuer, and B. W. Shore, Rev. Mod. Phys. **70**, 1003 (1998).
[4] B. Broers, H. B. van Linden van den Heuvell, and L. D. Noordam, Phys. Rev. Lett. **69**, 2062 (1992).
[5] M. O. Scully, S.-Y. Zhu, and A. Gavrielides, Phys. Rev. Lett. **62**, 2813 (1989).
[6] Y. Zhu, Phys. Rev. A **45**, R6149 (1992).
[7] M. Kasevich and S. Chu, Phys. Rev. Lett. **69**, 1741 (1992).
[8] K. Fujii, K. Higashida, R. Kato, and Y. Wada, e-print arXiv:quant-ph/0307066v2 (2003).
[9] S. E. Sklarz, D. J. Tannor, and N. Khaneja, Phys. Rev. A **69**, 053408 (2004).
[10] Q. Q. Wang, A. Muller, M. T. Cheng, H. J. Zhou, P. Bianucci and C. K. Shih, Phys. Rev. Lett. **95**, 187404 (2005).
[11] S. Rosenblum, S. Parkins, and B. Dayan, Phys. Rev. A **84**, 033854 (2011).
[12] J. Elgin, Phys. Lett. A **80**, 140 (1980).
[13] D. P. L Kancheva and S. Rashev, J. Phys. B **14**, 573 (1981).
[14] N. V. Vitanov, J. Phys. B **31**, 709 (1998).
[15] X.-s. Li and N.-y. BeiPhys. Lett. A **101**, 169 (1984).
[16] N. N. Bogolubov Jr., F. L. Kien, and A. S. Shumovsky, Phys. Lett. A **107**, 173 (1985).
[17] S.-y. Chu and D.-c. Chun, Phys. Rev. A **25**, 3169 (1982).
[18] E. Jaynes and F. Cummings, Proc. IEEE **51**, 89 (1963).
[19] G. Rempe, H. Walther, and N. Klein, Phys. Rev. Lett. **58**, 353 (1987).
[20] M. R. Nath, S. Sen, A. K. Sen and G. Gangopadhyay, Pramana **71**, 77 (2008).
[21] D. Braak, Phys. Rev. Lett. **107**, 100401 (2011).
[22] S. Haroche and J. M. Raimond, Adv. At. Mol. Phys. **20**, 351 (1985).
[23] L. A. Bloomfield, R. C. Stoneman, and T. F. Gallagher, Phys. Rev. Lett. **57**, 2512 (1986).
[24] H. K. Avetissian and G. F. Mkrtchian, Phys. Rev. A **66**, 033403 (2002).
[25] H. K. Avetissian, B. R. Avchyan, and G. F. Mkrtchian, Phys. Rev. A **74**, 063413 (2006).
[26] X. Zhang, H. Jiang, J. Rao, and B. Li, Phys. Rev. A **68**, 025401 (2003).
[27] X. Zhang, H. Jiang and J. Rao, J. Phys. B **36**, 4089 (2003).
[28] C. Jin, X. X. Zhou, and S. F. Zhao, Commun. Theor. Phys. **47**, 119 (2007).
[29] C. Jin, X. X. Zhou, and S. F. Zhao, Commun. Theor. Phys. **44**, 1065 (2005).
[30] Y.-L. He, Phys. Rev. A **84**, 053414 (2011).
[31] Y.-L. He, J. Phys. B **45**, 015001 (2012).